Construction and Building Materials 157 (2017) 372–381

Contents lists available at ScienceDirect

Construction and Building Materials

journal homepage: www.elsevier.com/locate/conbuildmat

A comparative study on mechanical properties of surface modified polypropylene (PP) fabric reinforced concrete composites

Guyu Feng, Xinyue Wang, Diantang Zhang, Haijian Cao, Kun Qian *, Xueliang Xiao

Key Laboratory of Science and Technology of Eco-Textiles, Ministry of Education, Jiangnan University, Wuxi 214122, China
College of Textile & Clothing, Jiangnan University, Wuxi 214122, China

HIGHLIGHTS

- Graft of AA and GO improves surface hydrophilicity and roughness of PP fabric, thereby improves interfacial properties between PP fabric and concrete.
- Graft of AA and Go improved flexural modulus and strength of PP fabric reinforced concrete.
- Modified PP fabric reinforced concretes show a more ductile mode of failure.
- Graft of AA and GO significantly improved the freeze-thaw resistance.

ARTICLE INFO

Article history:
Received 1 January 2017
Received in revised form 31 July 2017
Accepted 1 August 2017

Keywords:
PP fabric
Concrete
Graft
Mechanical property
Freeze-thaw durability

ABSTRACT

In this study, acrylic acid (AA) and grapheme oxide (GO) were grafted onto the surface of PP fabric in order to improve mechanical property and freeze-thaw durability of PP fabric reinforced concrete composites. Results showed that the successful graft of AA and GO increased the surface roughness of PP fabric as well as improved the hydrophilicity of PP fabric. Compressive property of modified PP fabric reinforced concrete composites showed slight increase. Flexural strength of PP-g-AA-GO fabric reinforced concrete composites increased by 25.6% compared with that of pristine PP fabric reinforced concrete composites. The addition of various PP fabrics in concrete significantly improved its freeze-thaw durability. PP-g-AA-GO fabric reinforced concrete composites achieved the highest relative dynamic modulus of elastic and residual flexural strength, as well as mass remaining percentage.

© 2017 Published by Elsevier Ltd.

1. Introduction

Cement based composite is one of the most widely used man-made composite materials in many fields, such as building, roadway, bridge and so on, due to its ultrahigh hardness and outstanding pressure resistance after setting [1]. Concrete, as typical cement based composite, is composed of cement as binder, coarse aggregate as framework, fine aggregate and fly ash as filler, as well as water and other agents. However, cracks and fissures usually appear on the surface of concrete when it is subjected to tensile or flexural loading due to its poor toughness, thereby resulting in the failure of concrete [2].

In order to remedy these defects in utility of applications, various reinforcements have been added into concrete. The development of steel reinforced concrete partly improved the situation. However, steel is vulnerable to corrosion which may result in structural damage of the concrete. Moreover, the steel industry often consumes a lot of energy and produces large amounts of greenhouse gases which may cause environmental damage [3]. Therefore, in recent years, chopped syntheticfibers, such as polyethylene (PE) [4], polyvinyl alcohol (PVA) [5], polyethylene terephthalate (PET) [6] and polypropylene (PP) have been added to concrete as reinforcement to enhance the mechanical and engineering properties of concrete. However, it is inevitable that short fibers randomly dispersed in the concrete when used to reinforce concrete. In this case there is a limitation in controlling the exact location of fibers inside the concrete. Finally, inevitable local aggregation and partially unoriented distribution of chopped syntheticfibers will cause the reduction of concrete effectiveness [7]. With the development of weaving technology, fiber-reinforced concrete has gradually been replaced by fabric-reinforced concrete. Fabric-reinforced concrete composites make up for deficiencies of both steel-reinforced concrete and fiber-reinforced concrete. On the one hand, fabric-reinforced concrete is corrosion resistant

* Corresponding author at: Key Laboratory of Science and Technology of Eco-Textiles, Ministry of Education, Jiangnan University, Wuxi 214122, China.
E-mail addresses: fengguyu890@163.com (G. Feng), qiankun_8@163.com (K. Qian).

https://doi.org/10.1016/j.conbuildmat.2017.08.004
0950-0618/© 2017 Published by Elsevier Ltd.

compared with steel-reinforced concrete, thus prolonging the service life and reducing the maintenance cost of the concrete composite [7]. On the other hand, fabrics have inimitable advantages and properties when used to reinforce concrete when compared with fibers. They can be placed in particular positions and directions subjected to tensile or flexural loadings [7], which allows for designing for specific characteristics as required by loading direction and magnitude, thereby promoting utilization efficiency of reinforcement and more favorable for improving mechanical and engineering property of fabric reinforced concrete composites. Therefore, fabric-reinforced concrete composites have widely potential application prospects in low-rise building, low-volume traffic roads and so on.

Nowadays, PP fabric is one of the most widely used reinforcements in concrete due to light weight, high strength and modulus, excellent abrasion resistance and corrosion resistance, as well as low cost [8]. Many scholars and researchers concentrate on PP fabric-reinforced concrete composites. Peled et al. [9] studied tensile properties of sandwich cement-based composites that combined different layers of single fabric types including PE, PP, AR glass and aramid.

The key factor for outstanding mechanical properties of fabric-reinforced concrete is the interfacial adhesion between fabric and concrete matrix [10]. However, the hydrophobic and smooth surfaces of PP fabric resulted in poor binding forces on fabric/concrete interface, which finally affected the concrete performance [11,12]. It is well known that the fabric/concrete interface can be effectively improved by means of surface treatment [13]. The modification on surface chemistry and morphology of fabrics can effectively increase the interfacial strength of fabric-reinforced concrete composites [14,15]. Many articles have been reported on kinds of surface treatment of PP fiber [16–18], however, there are few related to surface treatment of PP fabric. Acrylic acid (AA) is a surface-active-agent commonly used for improving surface activity of materials. Graphene oxide (GO) has large specific surface area on which exists a large amount of reactive hydrophilic groups, which is favorable for improving interfacial properties between fabric and concrete. Grafting AA and GO onto the surface of PP fiber has been reported by Wang et al. [19] and Li et al. [20]. However, there has no article reported on grafting AA and GO onto the surface of PP fabric before.

Hence, in the first stage of this study, acrylic acid (AA) was grafted onto the surface of PP fabric under UV radiation for different time to find a suitable grafting degree. After that, grapheme oxide (GO) was grafted onto the surface of PP-g-AA fabric by esterification reaction. The effects of AA and GO grafting reaction on the surface hydrophilicity of PP fabrics were investigated in detail by analyzing the changes in chemical component, surface composition, morphology, surface microscopic structure, and surface hydrophilicity of the fabrics. In the second stage, pristine PP fabric, modified PP-g-AA and PP-g-AA-GO fabrics were added into concrete for reinforcement. Mechanical properties and freeze-thaw durability of plain concrete and three types of fabric-reinforced concrete composites were measured and investigated in detail.

2. Experimental

2.1. Materials

PP fabrics were commercially available and purchased from Shandong Xinyu Geotechnical Engineering Materials Co. Ltd. (China) (fiber fineness is 300tex, warp density and weft density are 9/cm). Acrylic acid (AA), benzoyl peroxide(BPO), isopropyl alcohol(IPA), benzophenone (BP), thionyl chloride, acetic acid and acetone were provided by Sino Pharm Chemical Reagent Co. Ltd.(China) and used as received without further purification. The graphene oxide (GO) was purchased from Shanxi Fenghuiyuan Science and Technology Co. Ltd. (China). All chemical reagents used in the experiment were analytical pure grades.

2.2. Preparation of PP-g-AA-GO fabric

The fabrication process of PP-g-AA-GO fabric was shown in Fig. 1. Pristine PP fabric was soaked into acetone with supersonic vibration for 4 h to remove the impurities on fiber surface adequately before use. Step 1 was the process introducing the active sites onto PP backbone through the initiation of BPO [19]. PP fabric was soaked into a mold filled with 1.25 wt% BPO toluene solution for 0.5 h with temperature rising from 50 °C to 90 °C. After that, the toluene solution was removed by evaporation at 95 °C for 15 min. The treatment was carried out under nitrogen atmosphere.

In Step 2, the PP fabric was soaked into aqueous solution contain 20 wt% IPA as solvent, 0.5 wt% BP as initiator and 30 wt% AA. The grafting process was carried out under nitrogen atmosphere with the temperature of 60 °C for different time varied from 10 min to 90 min. The wave length of UV radiation was selected as 312 nm. After grafting process, unreacted monomer and homopolymer were removed from the samples by acetone extraction with supersonic vibration at room temperature for 4 h [20]. The PP-g-AA fabric samples with various grafting time were then obtained. The grafting degree of PP-g-AA fabrics were calculated and investigated to obtain a better process parameter for the next step.

Step 3 was the process grafting GO onto the surface of PP-g-AA fabric by esterification reaction. The PP-g-AA fabric was soaked into aqueous solution with 0.5 wt % GO, 6 wt% acetic acid as catalyst and 0.21 wt% thionyl chloride as dispersing agent. The mold was placed on the constant temperature shaker at 50 °C for 0.5 h, exposed to the air. Unreacted GO was removed from the sample by acetone extraction with supersonic vibration at room temperature for 4 h, and then dried at 60 °C to constant weight.

2.3. Concrete mixture design

Based on previous research and industry practice [3], standard mixture design for 25 MPa concrete used in this study is shown in Table 1. The grain-size distribution of fine sand, coarse sand and coarse aggregate used in this study is presented in Fig. 2. Concrete was homogeneously mixed in a concrete truck-mixer.

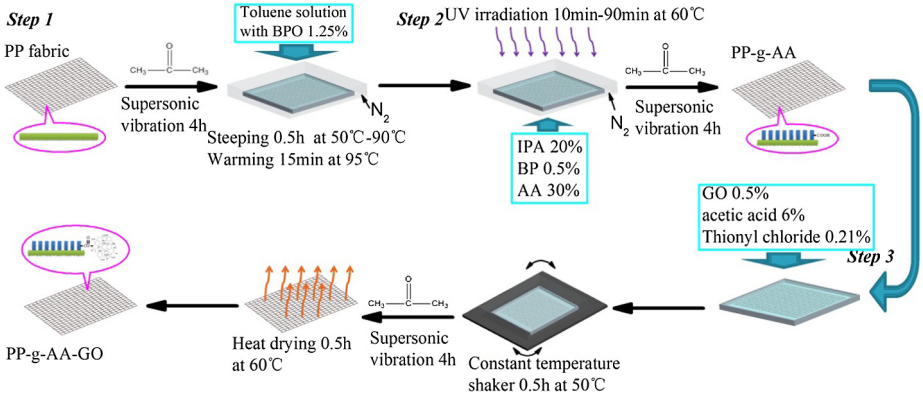

Fig. 1. Schematic illustration of fabrication process of PP-g-AA-GO fabric.

Table 1
Concrete mixture design.

Material	Content (kg/m^3)
0.075–0.6 mm fine sand	750
0.6–4.75 mm coarse sand	590
4.75–9.5 mm coarse aggregate	680
Fly ash	134
Cement	186
Cellulose	3
Air entrapment admixture (ml/100 kg)	22
Water (l/m^3)	116

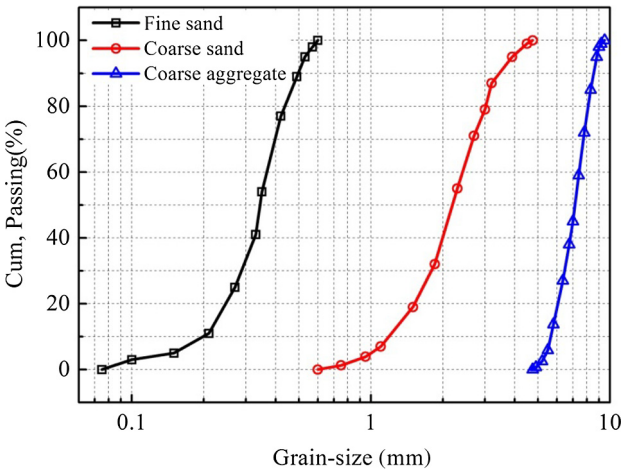

Fig. 2. Grain-size distribution of sand and aggregate.

2.4. Preparation of PP fabric-reinforced concrete composites

PP fabric reinforced concrete samples and plain concrete samples were casted by standard rodding compaction method with a concrete-fabric-concrete sandwich structure according to the Chinese specification GB/T 50081-2002. Three kinds of PP fabrics (pristine PP fabric, PP-g-AA fabric, PP-g-AA-GO fabric) with single layer were put in the middle of the concrete in order to investigate the effect of grafting of AA and GO on the mechanical and engineering properties of fabric reinforced concrete composites. After forming at room temperature for 24 h, all samples were taken out of the mold and then cured in saturated lime water until taken out for tests. Compressive and flexural samples are shown in Fig. 3. Put the fabric in the middle of the concrete provided the same function of retarding growth of cracks with other positions. Put the fabric in the middle of the concrete has no significant difference with other positions on provide mechanical properties and engineering properties of fabric reinforced concrete composites. Our work mainly focused on effect of various kinds of fabrics (single layer) on mechanical property and engineering property of fabric reinforced concrete composites. Therefore, we did not include the item—several layers in tour work.

3. Characterizations

3.1. FT-IR spectroscopy

The FT-IR measurement was performed using Nicolet iS10FT-IR spectrometer (Thermo Fisher Scientific, USA). The spectra were recorded in the range of 650–4000 cm^{-1}.

3.2. X-ray photoelectron spectroscopy (XPS)

XPS spectra were obtained by ESCALAB 250XI X-ray Photoelectron Spectroscopy (Thermo, USA) with MgKα X-ray source (200 W, 12 kV, $h\upsilon$ = 1486.6 eV). Survey spectra were recorded with pass energy of 50 eV, whereas selected atomic signals were acquired with 10 eV of pass energy. In the spectra, the position of the C—C/C—H was specified at 284.7 eV, and other peaks of different carbon environment were relative to this peak. The electron take-off angle from coatings was 90° from the surface. The C1s envelope was analyzed and peak-fitted after subtraction of a Shirley background using Gaussian-Lorenzian peak shapes.

3.3. Static water contact angle

The contact angle was measured using SL200B static contact angle/interfacial tension meter (Kino Industry Co. Ltd., USA) by

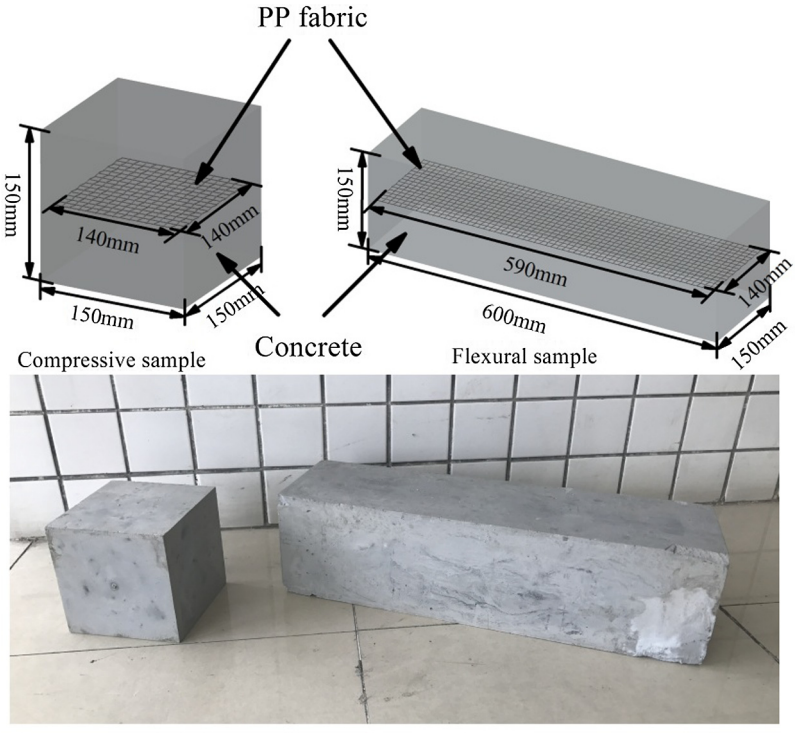

Fig. 3. Concrete samples for compressive and flexural tests.

sessile drop method. 5 μL deionized water droplets were gently deposited onto the fabric surface that conditioned to equilibrium moisture content at room temperature. Five seconds later dropping photos were taken with a high resolution camera and water contact angles were measured from photos. The mean and standard deviations were calculated from at least 5 tests for each sample.

3.4. Scanning electron microscope (SEM)

SEM images of PP fibers extracted from various PP fabrics were taken using SU1510 scanning electron microscope (Hitachi, Japan).

3.5. Atomic force microscope (AFM)

AFM images were taken using CSPM 4000 atomic force microscope (Benyuan Co. Ltd., China) in a tapping mode over a window of 2 μm × 2 μm. Each sample was fixed on a quartz plate with two pieces of adhesive tape on two ends of the sample.

3.6. Tensile test of PP fabric

Instron 3385H universal testing machine was used for tensile test of PP fabric before and after surface treatment. According to the Chinese specification GB/T 3923.1-2013, sample size was 250 mm in length and 50 mm in width. Tensile load versus deflection curves of various PP fabrics were measured with the gauge length of 200 mm and the crosshead speed of 100 mm/min.

3.7. Mechanical property

3.7.1. Compressive property

Compressive properties of PP fabric-reinforced concrete were measured using universal testing machine with a maximum load capacity of 5000 kN according to the Chinese specification GB/T 50081-2002. Compressive strength and modulus were measured respectively on the 7th, 14th, 21st and 28th day. The mean and standard deviations were calculated for $n = 3$. The compressive strength was calculated as the following equation:

$$f_{cc} = \frac{F}{A}$$

in which f_{cc} (MPa) is compressive strength; F (N) is fracture load; A (mm^2) is area of thrust surface. The modulus was obtained directly from the testing machine.

3.7.2. Flexural property

Flexural properties of concrete samples were measured using universal testing machine under four-point loading. Flexural strength and modulus were measured respectively on the 7th, 14th, 21st and 28th day, and the mean and standard deviations were calculated for $n = 3$ (three samples were tested for each case). The variations in the test results were shown in the form of error bar in Figs. 11–13. The schematic diagram of flexural test was shown in Fig. 4.The flexural strength was calculated as following equation:

$$f_f = \frac{Fl}{bh^2}$$

in which f_f (MPa) is flexural strength; F (N) is fracture load; l (mm) is span between two supports; b and h are width and height of the sample. The flexural modulus was obtained directly from testing machine. The maximum deflection was measured to analyze toughness of concrete sample.

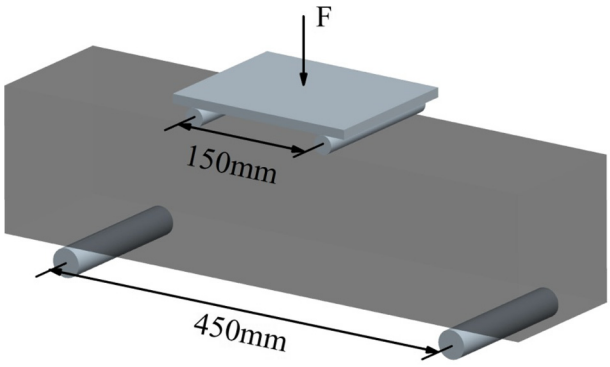

Fig. 4. Schematic diagram of flexural test.

3.8. Freeze-thaw test

Cyclic freeze-thaw tests were carried out to study the freeze-thaw resistance of PP fabric-reinforced concrete composites, referring to the Chinese specification GB/T 50082-2009. Specimens that reinforced with various forms of PP fabrics were subjected to repeated freezing and thawing cycles with a total 150 freeze-thaw cycles. The mass loss (ML), relative dynamic modulus of elastic (RDME) and residual flexural strength were measured every 25 cycles to evaluate the durability of the concrete samples. The relative dynamic modulus of elastic can be calculated according to the following equation:

$$E = \left(\frac{f_n^2}{f_1^2}\right) \times 100\%$$

where E is the relative dynamic modulus of elastic of the concrete specimens; f_n is fundamental transverse frequency after n freezing and thawing cycles and f_1 is initial fundamental transverse frequency. The residual flexural strength coefficient can be calculated with:

$$k_f = \left(\frac{\sigma_{nf}^R}{\sigma_f}\right) \times 100\%$$

where k_f is the residual flexural strength coefficient; σ_f^R is residual flexural strength after n freezing and thawing cycles; and σ_f is initial flexural strength.

The fundamental transverse frequencies of concrete specimens were tested by a cyclic forced resonance test instrument system. In the freeze-thaw study, the mass loss (ML), relative dynamic modulus of elastic (RDME) and residual flexural strength (RFS) of the plain concrete were designated as the reference value for the calculation and investigation of durability and stability for fabric reinforced concrete samples.

4. Results and discussion

4.1. Effect of grafting time on grafting degree

It is well known that grafting time has a major effect on grafting degree in a grafting reaction. In our work, the grafting degree is closely relevant to the weight increasing rate of PP fabric. Therefore, we calculated the grafting degree under different UV radiation time to investigate the effect of grafting time on grafting degree of AA. The grafting degree (G) was calculated as the following equation:

$$G(\%) = \frac{W_1 - W_0}{W_0} \times 100\%$$

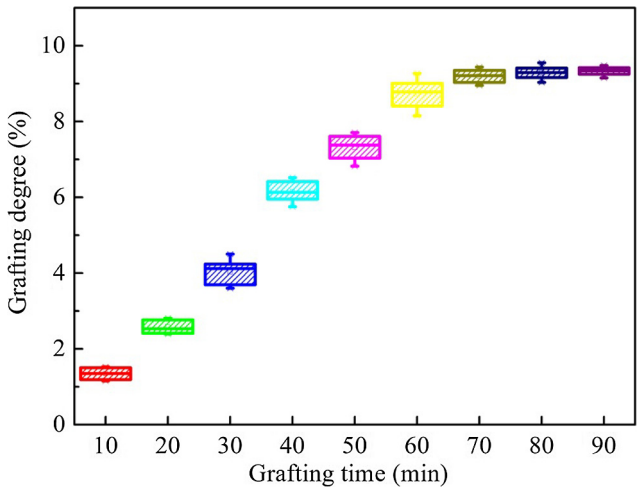

Fig. 5. Effect of grafting time on grafting degree.

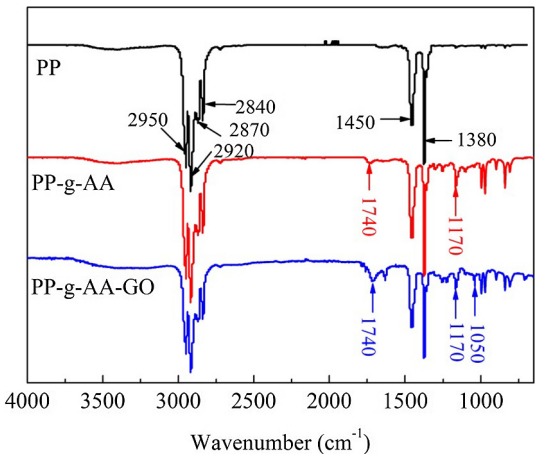

Fig. 6. FT-IR spectra of pristine PP fabric, modified PP-g-AA and PP-g-AA-GO fabrics.

in which W_0 is the weight of pristine PP fabric; W_1 is the weight of grafted PP fabrics. The curve of grafting degree versus UV radiation time is shown in Fig. 5. It is observed from Fig. 5 that the grafting degree increases with radiation time. The significant improvement in grafting degree indicated that massive active groups successfully grafted onto the surface of PP fabric. It is well supported by the equal reactivity theory in the radical polymerization [21]. Above the radiation time of 70 min, the grafting degree remained constant around 9.3%. The asymptotic saturation of the grafting degree was due to decomposition of BP and self-polymerization of AA [22–24].Therefore, a radiation time of 70 min was selected as the most suitable grafting time for subsequent experiment.

4.2. Chemical structures

Fourier transform infrared (FT-IR) spectroscopy was carried out to study the changes in chemical structures of PP fabric [25]. Fig. 6 shows the FT-IR spectra of pristine PP fabric, modified PP-g-AA fabric and PP-g-AA-GO fabric. The assignment of various wavelengths is presented in Table 2.

In the spectra of pristine PP fabric, peaks at 2950 and 2870 cm^{-1} are attributed to —CH_3 stretching vibration. Peaks at 2920 and 2840 cm^{-1} correspond to —CH_2 stretching vibration. Peaks at 1450 and 1380 cm^{-1} are related to —CH_3 bending vibration [26]. In the spectra of PP-g-AA fabric, peaks at 1740 and 1170 cm^{-1} are assigned to C=O stretching vibration of carboxyl and —OH stretching vibration of carboxyl, respectively [27], indicating that AA has been successfully grafted onto the surface of PP fabric [28]. As for the spectra of PP-g-AA-GO fabric, peak at 1050 cm^{-1} is related to —O=C—O bending vibration [29], indicating that GO has been successfully grafted onto the surface of PP-g-AA fabric. FT-IR spectra confirm the successful graft of AA and GO onto the surface of PP fabric. Further surface chemical information of pristine PP fabric, modified PP-g-AA fabric and PP-g-AA-GO fabric were investigated by XPS analysis.

4.3. Surface composition

XPS measurement was carried out to further investigate the distribution of various functional groups on the surface of modified PP fabrics. Fig. 7(a) shows the XPS wide-scan spectra of pristine and modified PP fabrics, and the inset is O1s:C1s ratios. Pristine PP fabric shows almost no oxygen content with the O1s:C1s ratio of around 0. The ratio increased from 0 to 0.36 after grafting AA onto the surface of PP fabric and eventually reached 0.69 after grafting

Table 2
Assignment of wavelengths.

Wavelength (cm^{-1})	Functional group assignment
2950 cm^{-1} and 2870 cm^{-1}	—CH_3 stretching vibration
2920 cm^{-1} and 2840 cm^{-1}	—CH_2 stretching vibration
1450 cm^{-1} and 1380 cm^{-1}	—CH_3 bending vibration
1740 cm^{-1}	—C=O stretching vibration of carboxyl
1170 cm^{-1}	—OH stretching vibration of carboxyl
1050 cm^{-1}	—O=C—O bending vibration

GO onto the surface of PP-g-AA fabric [30]. The increase in oxygen content on the surface of PP fabric is attributed to the introduction of oxygen-containing groups. Deconvolution of C1s core level spectra of pristine and modified PP fabrics are shown in Fig. 7(b)–(d). In pristine PP fabric (Fig. 7(b)), only one component was observed at 284.8 eV originated from C—C/C—H [18,31]. After grafting AA and GO onto the surface of PP fabric, three newly appeared components at 287.7 eV, 285.9 eV and 288.7 eV were assigned to C—COOH, C—OH, and C—COO, respectively [18]. The atomic percentage of C—COOH on the surface of PP-g-AA fabric was only 3 at.%, but the percentage dramatically increased to 27 at.% after grafting GO onto PP-g-AA fabric. Meanwhile, the atomic percentage of C—OH finally reached 10.3 at.% on the surface of PP-g-AA-GO fabric. These changes indicate that numerous hydrophilic groups have been grafted onto the surface of PP fabric, consistent with observations in FT-IR spectra [30]. The introduction of numerous hydrophilic groups will certainly improve the surface hydrophilicity of PP fabric, thereby leading to enhancement in mechanical and engineering properties. The surface element compositions and functional group compositions of various PP fabrics are shown in Table 3.

4.4. Morphology

Changes in chemical structures and surface compositions will certainly influence morphology. Therefore, SEM and AFM measurements were carried out to investigate effects of grafting on morphology of PP fabrics. Fig. 8 shows SEM images of fibers extracted from pristine PP fabric, modified PP-g-AA and PP-g-AA-GO fabrics, respectively. It was observed from Fig. 8 that the surface of pristine PP fiber was smooth. After graft of AA, thin layer of AA molecule embossment was clearly seen on the surface of PP-g-AA fiber, thereby increasing the surface roughness of PP fabric. Increase in surface roughness helped to increase the specific surface area of PP fabric, which was favorable for the subsequent graft of GO. After graft of GO, numerous GO particles were

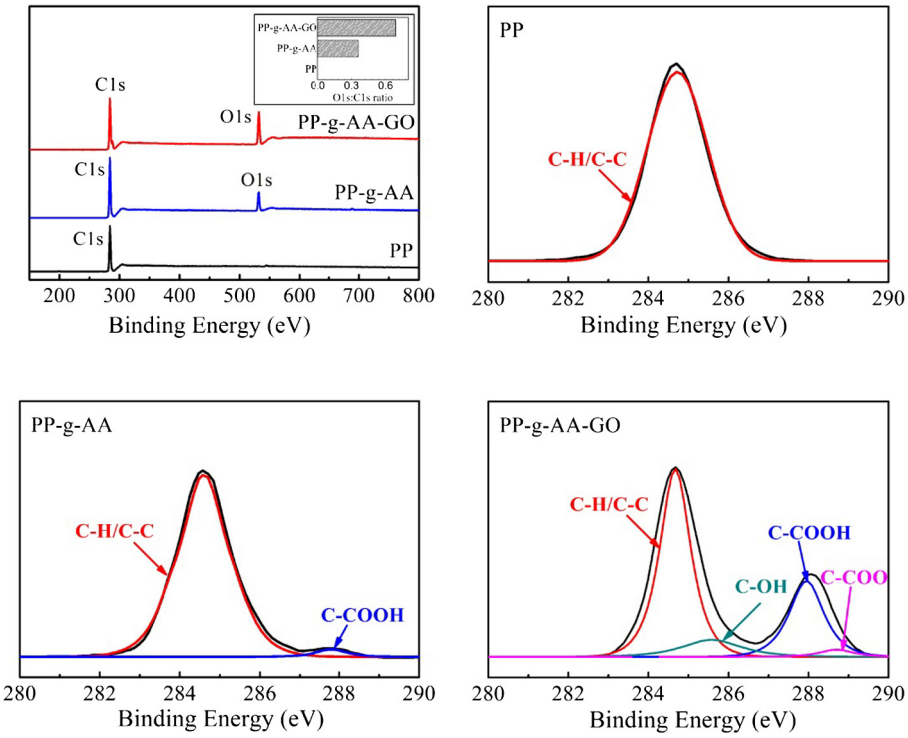

Fig. 7. XPS spectra and C1s peak-fitting curves of pristine PP fabric, modified PP-g-AA and PP-g-AA-GO fabrics.

Table 3
Surface element compositions and functional group compositions of various PP fabrics.

Samples	Element composition (%)		Functional group composition (%)			
	C1s	O1s	C—C/C—H	C—OH	C—COOH	C—COO
Pristine PP	100	0	100	–	–	–
PP-g-AA	73.5	26.5	97	–	3	–
PP-g-AA-GO	59.2	40.8	60.2	10.3	27	2.5

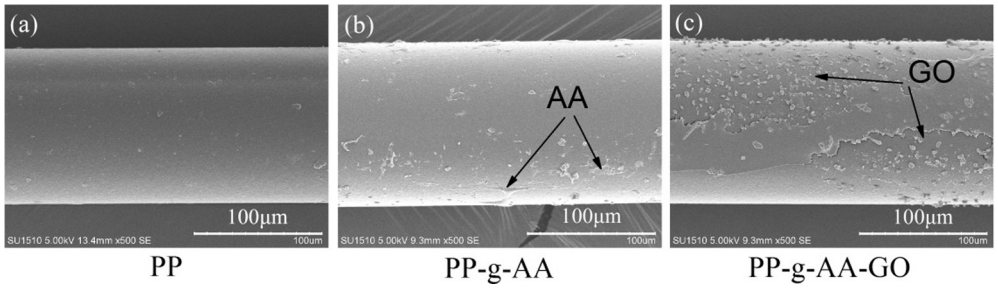

Fig. 8. SEM images of various PP fibers extracted from pristine PP fabric, modified PP-g-AA and PP-g-AA-GO fabrics, respectively.

observed uniformly distributed on the surface of PP-g-AA fiber (Fig. 8(c)). The successful graft of GO helped to improve the surface hydrophilicity of PP fabric thereby significantly improving interfacial properties between fabric and concrete and in turn led to enhancement in mechanical properties of PP fabric-reinforced concrete. SEM images revealed that AA and GO had been successfully grafted onto the surface of PP fabric. In order to obtain more microscale information about the effect of graft on the surface morphology of PP fabric, AFM height images corresponding to SEM images were shown in Fig. 9. The root-mean-square roughness of pristine PP fiber was 3.71 ± 0.35 nm, which increased to 28.72 ± 5.35 nm and then 49.79 ± 7.84 nm after graft of AA and GO, respectively, indicating that the surface of PP fabric became rougher after graft. This was consistent with the observations in SEM images.

4.5. Surface hydrophilicity

Static water contact angle (SWCA) measurement was carried out to study the effect of graft on the surface wettability of PP fabric. Fig. 10 showed the static WCA images. The change in static water contact angle could be observed after each step of graft. The pristine PP fabric was intrinsically hydrophobic with a wetting angle of around 77° ± 3.7°. After graft with acrylic acid, the wetting angle of PP-g-AA fabric slightly decreased to 64.1° ± 2.1° due to the

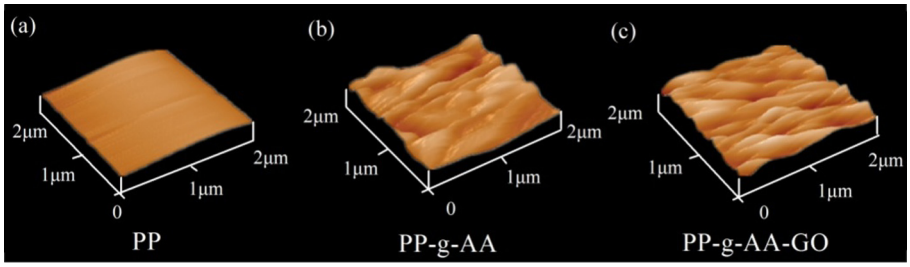

Fig. 9. AFM images of various PP fibers extracted from pristine PP fabric, modified PP-g-AA and PP-g-AA-GO fabrics, respectively.

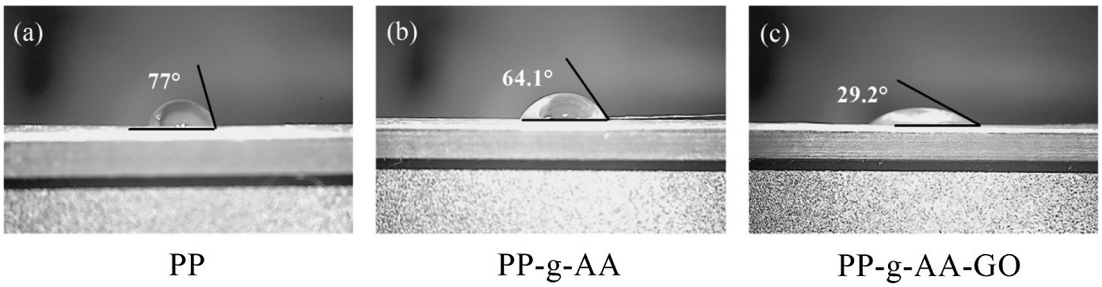

Fig. 10. Static water contact angle images of pristine PP fabric, modified PP-g-AA and PP-g-AA-GO fabrics.

introduction of hydrophilic carboxyl groups. The wetting angle of PP-g-AA-GO fabric finally decreased to 29.2° ± 1.3° after graft of GO, indicating the improvement in surface hydrophilicity of PP fabric due to the introduction of hydrophilic groups including carboxyl groups and hydroxyl groups. SWCA results showed that the graft significantly improved the surface hydrophilicity of PP fabric [16], which could help to improve the interfacial properties between PP fabric and concrete, and might in turn lead to enhancement in mechanical and engineering properties of PP fabric-reinforced concrete.

4.6. Tensile properties of PP fabric

The tensile load versus deflection curves of various PP fabrics were shown in Fig. 11. There are no obvious difference in strengths, elongations and modulus of various PP fabrics, indicating that the improvement in surface activity of PP fabric has no direct effect on tensile properties of PP fabric.

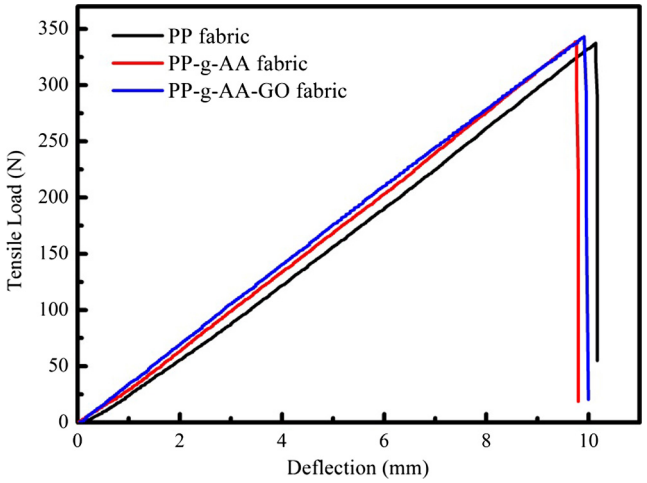

Fig. 11. Tensile load versus deflection curves of various PP fabrics.

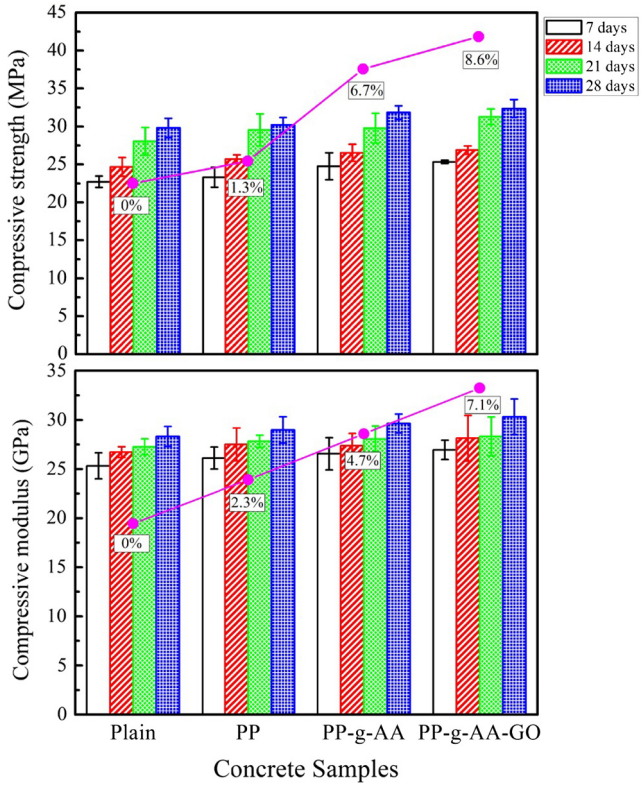

Fig. 12. Compressive properties of various PP fabrics reinforced concrete samples.

4.7. Mechanical property

4.7.1. Compressive property

The compressive strength and modulus of various PP fabrics reinforced concrete samples as well as a plain concrete sample were shown in Fig. 12. The relative ratio represents the increase rate for the concrete samples comparing to the reference sample (the plain concrete).

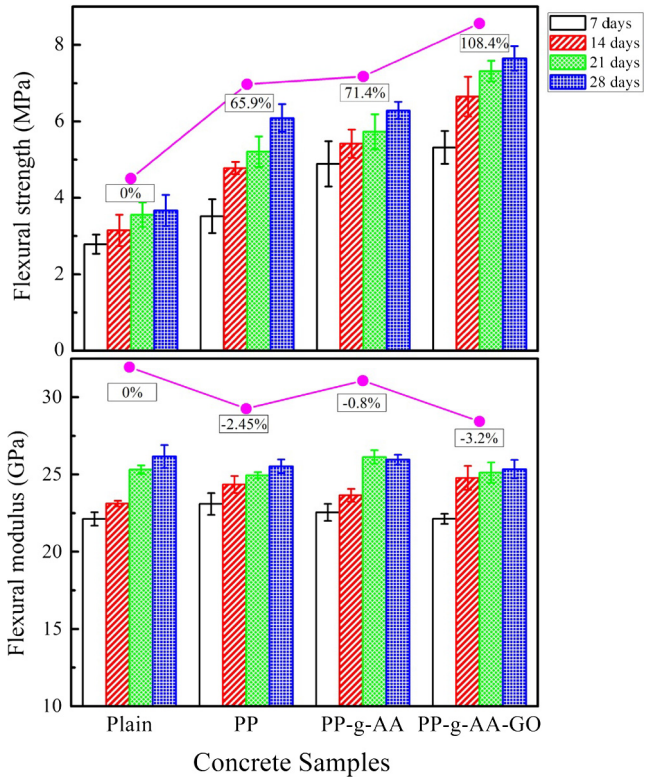

Fig. 13. Flexural properties of various PP fabrics reinforced concrete samples.

It was observed from Fig. 12 that the addition of pristine PP fabric showed no obvious effect on compressive strength of PP fabric reinforced concrete samples [32]. There is no obvious increase in compressive strength compared with that of plain concrete, which has also been confirmed by Wu et al. [33]. This is due to poor interfacial properties between pristine PP fabric and concrete. While modified PP fabrics reinforced concrete samples showed larger compressive strength, which is probably due to the enhancement in the interfacial properties. Grafting AA and GO onto the surface of PP fabric significantly improved the surface hydrophilicity of PP fabric due to the introduction of oxygenous groups, thus leading to enhancement in interfacial properties between fabric and concrete, and finally improved the compressive strength of fabric reinforced concrete composites. On the other hand, PP fabric plays the role of redistributing compressive load in the concrete [34]. A closer combination will certainly help to dissipate load more effectively thereby increasing the compressive strength of the integral fabric-reinforced concrete. These results well confirmed previous hypothesis that modified PP fabric-reinforced concrete had higher mechanical properties than pristine PP fabric reinforced-concrete.

4.7.2. Flexural property

The variation in flexural strength and modulus of various fabric-reinforced concrete samples are shown in Fig. 13. There is a significant increase in flexural strength of pristine PP fabric-reinforced concrete compared with that of plain concrete, with the value increases by 65.9%. The concrete cracking behavior was delayed due to the addition of PP fabric which changed cracking direction and thus decelerating the cracking. When cracks developed up to the interface between PP fabric and concrete, the growth direction of cracks could be changed from vertical direction to horizontal direction along the interface. Furthermore, good interfacial properties often lead to excellent mechanical properties in fabric-reinforced concrete. Therefore, it is vital to improve interfacial properties in order to increase flexural strength of fabric-reinforced concrete.

Compared with the flexural strength of pristine PP fabric reinforced concrete, that of PP-g-AA fabric and PP-g-AA-GO fabric reinforced concrete increased by 3.3% and 25.6%, respectively. This could be attributed to the enhancement in interfacial properties due to the graft of AA and GO, which introduced numerous oxygenous groups onto the surface of PP fabric and improved the surface hydrophilicity of PP fabric. The integrity of fabric-reinforced concrete was also improved due to a tighter combination resulted from better interfacial property which decelerated the development of cracks along horizontal direction.

It was also observed form Fig. 13 that the flexural elastic modulus had no obvious change, indicating that the addition of PP fabric had no significant influence on the stiffness of fabric reinforced concrete. It is well known that the determinants of elastic modulus are bond strengths between atoms, molecules or ions [35]. Elastic deformation of concrete occurs when bond length and angle between atoms, molecules or ions of components in concrete changes [36]. However, the addition of PP fabric didn't change these factors during elastic deformation. Therefore, no obvious

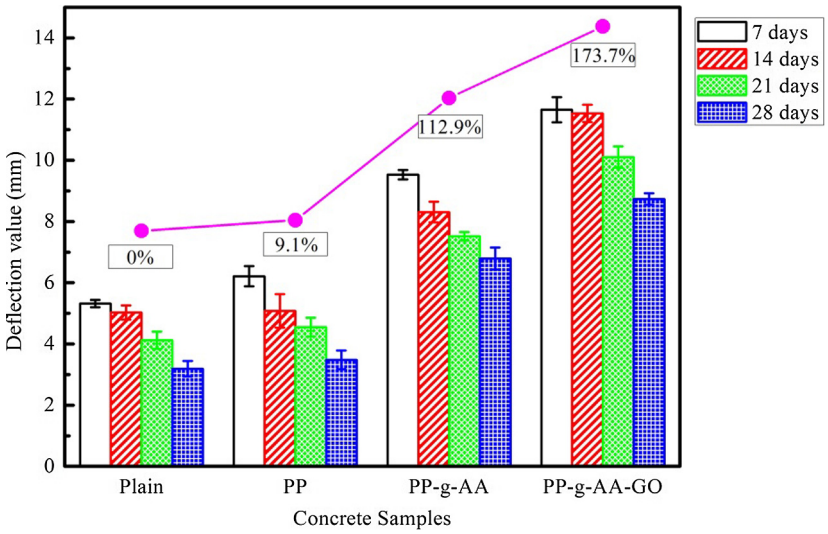

Fig. 14. Deflection of various PP fabrics reinforced concrete samples.

change in flexural elastic modulus was observed among various PP fabric reinforced concrete samples.

Deflection at maximum flexural load represents the concrete toughness, and the results are shown in Fig. 14. It was clearly observed that improvement in surface hydrophilicity of PP fabric significantly increased the toughness of fabric reinforced concrete samples. In other words, PP-g-AA-GO fabric reinforced concrete sample is the most ductile and least stiff one among various fabrics reinforced concrete samples. It should also be noted that during flexural tests, various PP fabrics reinforced concrete failed with numerous minor surface cracks, while the plain concrete failed catastrophically with large single cracks [3]. That is to say, fabric reinforced concrete demonstrated a relatively more ductile mode of failure. In the long run, modified PP fabric reinforced concrete could bear higher deformation without collapse [37] compared with plain concrete. Hence using modified PP fabric reinforced concrete as basic building materials will open up avenues for many applications in the future.

4.8. Freeze-thaw resistance

The typical mass loss curves of PP fabric-reinforced concrete composites under repeated freezing and thawing cycles are shown in Fig. 15. From Fig. 15, it is obviously observed that the weight gradually decreases with increasing freeze-thaw cycles. At the beginning of the freeze-thaw test (before 75 cycles), no obvious mass loss was observed. However, after about 75 cycles, much faster mass loss could be observed on all samples. After 150 freeze-thaw cycles, the mass remaining percentage of PP-g-AA-GO reinforced concrete samples reached 89.2%, while that of the plain concrete sample was only 84.2%. This indicated that the addition of PP fabrics reduced internal damage of concrete samples due to enhancing the previously weak bond between different components inside concrete. The higher integrity thereby resulted in better overall performance of PP fabric reinforced concrete samples. According to the mass loss results, it is concluded that additional PP fabrics in the concrete samples provided positive effect on their freezing and thawing resistances. The samples without PP fabrics suffered larger mass loss compared with the samples with PP fabrics added. In addition, variation in the forms of the additional PP fabrics did not significantly affect the mass loss percentage of PP fabric reinforced concrete composites.

The change of RDME of concrete samples is show in Fig. 16a. Although mass loss of concrete samples was slight at the beginning of the freeze-thaw cycles (before 75 cycles), reductions on RDME were still detected. This indicated that internal structural damage had already arose and developed in the concrete samples and thereby resulted in deteriorations on the stability of concrete. In addition, PP-AA-GO fabric reinforced concrete samples show the highest RDME value, indicating that the surface treatment effectively improved the RDME value due to the improvement in the integrity of concrete samples.

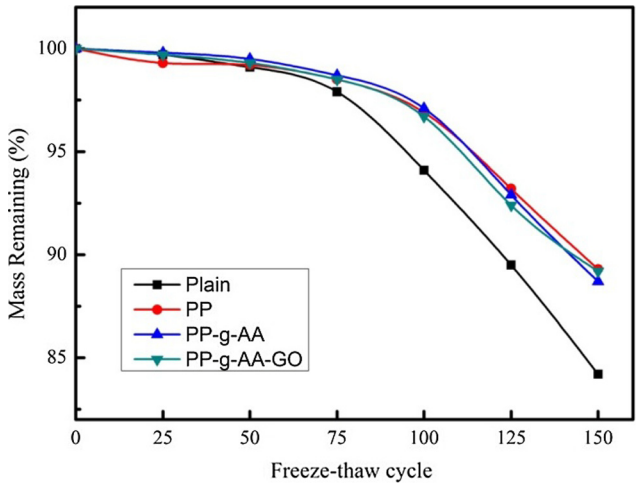

Fig. 15. Mass loss curves of various PP fabrics reinforced concrete samples.

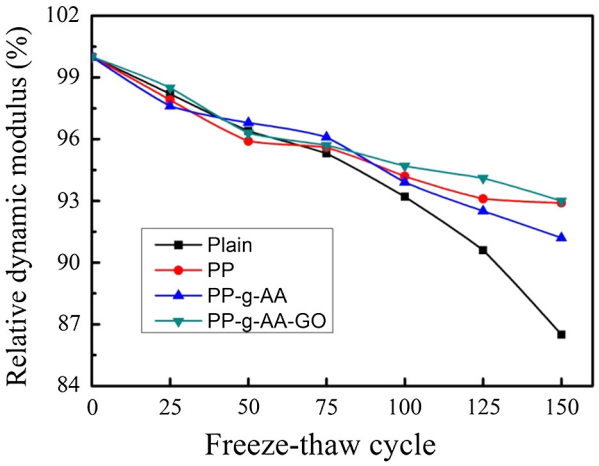

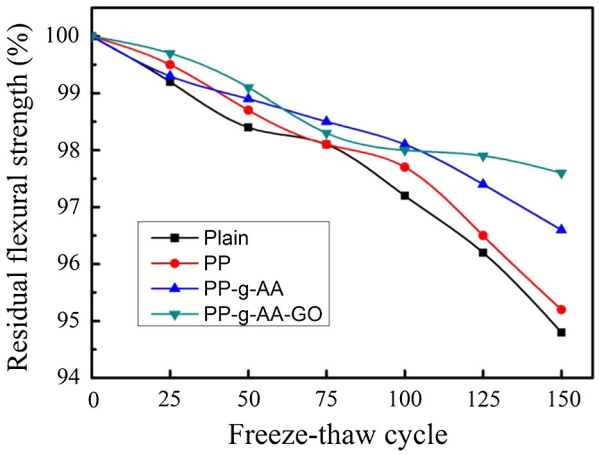

Fig. 16. RDME and residual flexural strength of various PP fabrics reinforced concrete samples.

The residual flexural strength of various concrete samples were also measured to investigate the stability of concrete samples, and the results were shown in Fig. 16b. From Fig. 16b, it is clearly observed that the residual flexural strength significantly reduced at the beginning of the test, which is consistent with the variation trends of the RDME. This further indicated the arising and development of the internal damage of concrete samples. It is also observed from Fig. 16b that compared with the plain concrete sample, fabrics reinforced concrete samples show higher residual flexural strength. Moreover, PP-AA-GO fabric reinforced concrete has the highest residual flexural strength among the three forms of concrete samples, which indicates that better interfacial property is favorable for the durability and stability of fabric reinforced concrete samples.

5. Conclusions

Surface hydrophilic modification of PP fabric was successfully conducted by grafting the AA and GO onto the surface of PP fabric

under UV radiation. This method introduced active groups onto the surface of PP fabric and changed the chemical activity of PP fabric, thereby improving interfacial property between PP fabric and concrete matrix, and finally improved mechanical and engineering properties of PP fabric reinforced concrete composites.

Based on the current results, the following conclusions could be acquired:

- The maximum grafting degree of AA was 9.3%, with the grafting time of 70 min, under 312 nm UV radiation at 60 °C.
- The FTIR and XPS results proved that AA and GO have been successfully grafted onto the surface of PP fabric.
- Graft of AA and GO increased the surface roughness of PP fabric.
- Graft of AA and GO significantly improved the surface hydrophilicity of PP fabric due to introduction of carboxyl groups and hydroxyl groups.
- Fabric category had no obvious influence on compressive strength and modulus of PP fabric reinforced concrete.
- Compared with the flexural strength of pristine PP fabric reinforced concrete, the flexural strength of PP-g-AA and PP-g-AA-GO fabrics reinforced concrete increased by 3.3% and 25.6%, respectively. However, graft of AA and GO shows no obvious effect on flexural elastic modulus of fabric reinforced concrete.
- The concrete toughness increased with the improvement in surface hydrophilicity of PP fabric.
- The addition of various categories of PP fabrics significantly improved the freeze-thaw durability of concrete. The concrete reinforced with PP-g-AA-GO fabric achieved the highest relative dynamic modulus of elastic (RDME) and residual flexural strength, as well as mass remaining percentage.

Acknowledgements

This work was supported by the National Key Research and Development Program of China (2016YFC-0304301 & 2016YFB0303200), Cooperative Innovation Fund-Prospective Project of Jiangsu Province (No. BY2015019-33). These projects also contributed a lot to our work. Project Name: Postgraduate Research & Practice Innovation Program of Jiangsu Provence. Project Number: KYCX17_1442 & KYCX17_1439.

References

[1] W. Zhang, N. Zhang, Y. Zhou, Effect of flexural impact on freeze-thaw and deicing salt resistance of steel fiber reinforced concrete, Mater. Struct., 1–8.
[2] P. Lura, G.P. Terrasi, Reduction of fire spalling in high-performance concrete by means of superabsorbent polymers and polypropylene fibers: small scale fire tests of carbon fiber reinforced plastic-prestressed self-compacting concrete, Cem. Concr. Compos. 49 (2014) 36–42.
[3] S. Yin, R. Tuladhar, J. Riella, D. Chung, T. Collister, M. Combe, N. Sivakugan, Comparative evaluation of virgin and recycled polypropylene fibre reinforced concrete, Constr. Build. Mater. 114 (2016) 134–141.
[4] S. Wang, H.T.N. Le, L.H. Poh, H. Feng, M.H. Zhang, Resistance of high-performance fiber-reinforced cement composites against high-velocity projectile impact, Int. J. Impact Eng. 95 (2016) 89–104.
[5] M. Sahmaran, I.O. Yaman, Hybrid fiber reinforced self-compacting concrete with a high-volume coarse fly ash, Constr. Build. Mater. 21 (1) (2007) 150–156.
[6] D. Foti, Preliminary analysis of concrete reinforced with waste bottles PET fibers, Constr. Build. Mater. 25 (4) (2011) 1906–1915.
[7] J. Hegger, S. Voss, Investigations on the bearing behaviour and application potential of textile reinforced concrete, Eng. Struct. 30 (7) (2008) 2050–2056.
[8] J. Yahaghi, Z.C. Muda, S.B. Beddu, Impact resistance of oil palm shells concrete reinforced with polypropylene fibre, Constr. Build. Mater. 123 (2016) 394–403.
[9] A. Peled, B. Mobasher, Z. Cohen, Mechanical properties of hybrid fabrics in pultruded cement composites, Cem. Concr. Compos. 31 (9) (2009) 647–657.
[10] A.K. Mohanty, L.T. Drzal, M. Misra, Engineered natural fiber reinforced polypropylene composites: influence of surface modifications and novel powder impregnation processing, J. Adhes. Sci. Technol. 16 (8) (2002) 999–1015.
[11] S.D. Lee, M. Sarmadi, F. Denes, J.L. Shohet, Surface modification of polypropylene under argon and oxygen-RF-plasma conditions, Plasmas Polym. 2 (3) (1997) 177–198.
[12] S. Singh, A. Shukla, R. Brown, Pullout behavior of polypropylene fibers from cementitiousmatrix, Cem. Concr. Res. 34 (10) (2004) 1919–1925.
[13] C. Zhang, V.S. Gopalaratnam, H.K. Yasuda, Plasma treatment of polymeric fibers for improved performance in cement matrices, J. Appl. Polym. Sci. 76 (14) (2000) 1985–1996.
[14] A. Bentur, S. Mindess, G. Vondran, Bonding in polypropylene fibre reinforced concretes, Cem. Concr. Compos. 11 (3) (1989) 153–158.
[15] F. Denes, D. Feldman, Z.Q. Hua, Z. Zheng, R.A. Young, Cementitious-matrix composites from $SiCl_4$-plasma-activated polypropylene fibres, J. Adhes. Sci. Technol. 10 (1) (1996) 61–77.
[16] B. Felekoglu, K. Tosun, B. Baradan, A comparative study on the flexural performance of plasma treated polypropylene fiber reinforced cementitious composites, J. Mater. Process Technol. 209 (11) (2009) 5133–5144.
[17] A.M. López-Buendía, M.D. Romero-Sánchez, V. Climent, C. Guillem, Surface treated polypropylene (PP) fibres for reinforced concrete, Cem. Concr. Res. 54 (2013) 29–35.
[18] Y. Zhao, W. Sun, S. Shi, Y. Gong, Biomimetic surface modification of polypropylene by surface chain transfer reaction based on mussel-inspired adhesion technology and thiol chemistry, Appl. Surf. Sci. (2016).
[19] W. Wang, L. Wang, X. Chen, Q. Yang, T. Sun, J. Zhou, Study on the graft reaction of poly (propylene) fiber with acrylic acid, Macromol. Mater. Eng. 291 (2) (2006) 173–180.
[20] S. Li, J. Wei, H. Yang, L. Wang, A. Wang, Y. Zhang, Y. Nie, A novel sorbent prepared by two-step grafting of acrylic acid and methyl methacrylate monomer onto a polypropylene matrix, Polym. Plast. Technol. 52 (5) (2013) 427–432.
[21] N.V. Tsarevsky, K. Matyjaszewski, "Green" atom transfer radical polymerization: from process design to preparation of well-defined environmentally friendly polymeric materials, Chem. Rev. 107 (6) (2007) 2270–2299.
[22] A.E.H. Ali, H.A. Shawky, M.H. El-Sayed, H. Ibrahim, Radiation synthesis of functionalized polypropylene fibers and their application in the treatment of some water resources in western desert of Egypt, 63 (1) (2008) 69–76.
[23] S.A. Gürsel, A. Wokaun, G.G. Scherer, Influence of reaction parameters on grafting of styrene into poly (ethylene-alt-tetrafluoroethylene) films, Nucl. Instrum. Methods Phys. Res., Sect. B 265 (1) (2007) 198–203.
[24] H. Kawakita, K. Uezu, S. Tsuneda, K. Saito, M. Tamada, T. Sugo, Recovery of Sb (V) using a functional-ligand-containing porous hollow-fiber membrane prepared by radiation-induced graft polymerization, Hydrometallurgy 81 (3) (2006) 190–196.
[25] A. Dong, Y. Yu, J. Yuan, Q. Wang, X. Fan, Hydrophobic modification of jute fiber used for composite reinforcement via laccase-mediated grafting, Appl. Surf. Sci. 301 (2014) 418–427.
[26] R. Morent, N. De Geyter, C. Leys, L. Gengembre, E. Payen, Comparison between XPS-and FTIR-analysis of plasma-treated polypropylene film surfaces, Surf. Interface Anal. 40 (3–4) (2008) 597–600.
[27] Z. Yuan, H. Tai, Z. Ye, C. Liu, G. Xie, X. Du, Y. Jiang, Novel highly sensitive QCM humidity sensor with low hysteresis based on graphene oxide (GO)/poly (ethyleneimine) layered film, Sens. Actuators, B 234 (2016) 145–154.
[28] J.M. Yang, H.T. Lin, T.H. Wu, C.C. Chen, Wettability and antibacterial assessment of chitosan containing radiation-induced graft nonwoven fabric of polypropylene-g-acrylic acid, J. Appl. Polym. Sci. 90 (5) (2003) 1331–1336.
[29] T. Wang, J. Lu, L. Mao, Z. Wang, Electric field assisted layer-by-layer assembly of graphene oxide containing nanofiltration membrane, J. Membr. Sci. (2016).
[30] H. Zhang, R. Deng, H. Wang, Z. Kong, D. Dai, Z. Jing, Y. Hou, Reduction of bromate from water by zero-valent iron immobilized on functional polypropylene fiber, Chem. Eng. J. 292 (2016) 190–198.
[31] Y. Liu, Y. Fang, J. Qian, Z. Liu, B. Yang, X. Wang, Bio-inspired polydopamine functionalization of carbon fiber for improving the interfacial adhesion of polypropylene composites, RSC Adv. 5 (130) (2015) 107652–107661.
[32] S. Kothandaraman, S. Kandasamy The effect of controlled permeable formwork liner on the mechanical properties of concrete, Mater. Struct., 1–11.
[33] H. Wu, Z. Liu, B. Sun, J. Yin, Experimental investigation on freeze-thaw durability of Portland cement pervious concrete (PCPC), Constr. Build. Mater. 117 (2016) 63–71.
[34] V. Corinaldesi, A. Nardinocchi, Mechanical characterization of engineered cement-based composites prepared with hybrid fibres and expansive agent, Compos. Part B 98 (2016) 389–396.
[35] S.B. Kim, N.H. Yi, H.Y. Kim, J.H.J. Kim, Y.C. Song, Material and structural performance evaluation of recycled PET fiber reinforced concrete, Cem. Concr. Compos. 32 (3) (2010) 232–240.
[36] A. Çavdar, Investigation of freeze–thaw effects on mechanical properties of fiber reinforced cement mortars, Compos. Part B 58 (2014) 463–472.
[37] R. Mishra, J. Militky, N. Gupta, R. Pachauri, B.K. Behera, Modelling and simulation of earthquake resistant 3D woven textile structural concrete composites, Compos. Part B 81 (2015) 91–97.